Decidual NK cells kill Zika virus–infected trophoblasts

Sumit Sen Santara[a,1], Ângela C. Crespo[a,b,1], Sachin Mulik[a,1,2], Cristian Ovies[a], Selma Boulenouar[c], Jack L. Strominger[b], and Judy Lieberman[a,3]

[a]Program in Cellular and Molecular Medicine, Boston Children's Hospital and Department of Pediatrics, Harvard Medical School, Boston, MA 02115; [b]Department of Stem Cell and Regenerative Medicine, Harvard University, Cambridge, MA 02138; and [c]Department of Neurology, Brigham and Women's Hospital, Harvard Medical School, Boston, MA 02115

Contributed by Judy Lieberman, October 11, 2021 (sent for review August 22, 2021; reviewed by Marco Colonna and Carolyn B. Coyne)

Zika virus (ZIKV) during pregnancy infects fetal trophoblasts and causes placental damage and birth defects including microcephaly. Little is known about the anti-ZIKV cellular immune response at the maternal–fetal interface. Decidual natural killer cells (dNK), which directly contact fetal trophoblasts, are the dominant maternal immune cells in the first-trimester placenta, when ZIKV infection is most hazardous. Although dNK express all the cytolytic molecules needed to kill, they usually do not kill infected fetal cells but promote placentation. Here, we show that dNK degranulate and kill ZIKV-infected placental trophoblasts. ZIKV infection of trophoblasts causes endoplasmic reticulum (ER) stress, which makes them dNK targets by down-regulating HLA-C/G, natural killer (NK) inhibitory receptor ligands that help maintain tolerance of the semiallogeneic fetus. ER stress also activates the NK activating receptor NKp46. ZIKV infection of *Ifnar1*$^{-/-}$ pregnant mice results in high viral titers and severe intrauterine growth restriction, which are exacerbated by depletion of NK or CD8 T cells, indicating that killer lymphocytes, on balance, protect the fetus from ZIKV by eliminating infected cells and reducing the spread of infection.

ZIKV | decidual NK | extravillous trophoblast | pregnancy | ER stress

In the first trimester of human pregnancy, when Zika virus (ZIKV) infection is most damaging to the developing fetus (1–3), ∼70% of maternal immune cells at the maternal–fetal interface are decidual natural killer cells (dNK), which are in close contact with extravillous trophoblasts (EVT), placental cells of fetal origin which invade the decidua to orchestrate placentation. T lymphocytes and natural killer (NK) cells generally do not kill EVT, which do not express the main classical HLA molecules responsible for T cell activation (HLA-A and B) (4–7) but do express HLA-C and nonclassical HLA-E and -G, which help inhibit NK cell activation. HLA-G, whose expression is mostly restricted to the placenta, helps maintain dNK tolerance of fetal cells. There is important cross-talk between dNK and EVT—EVT regulate the maturation of dNK precursor cells into tolerant dNK (8) and dNK promote EVT migration and invasion of spiral arteries, processes essential for placentation (9–13). Invading fetal EVT are susceptible to infection by a variety of pathogens, including human cytomegalovirus (HCMV), *Toxoplasma gondii*, and ZIKV (1, 14–17). dNK in the placenta face a difficult problem—they must tolerate the semiforeign fetus but still protect against infection. Although dNK contain the machinery needed to recognize and kill, they have reduced cytolytic activity against classical NK target cells recognized by peripheral blood NK cells (pNK) and are not known to kill infected trophoblasts (18–23). However, dNK degranulate and secrete cytokines, including interferon (IFN)-γ, in response to HCMV-infected maternal decidual stromal cells in equal levels to pNK (19, 20). We recently demonstrated that dNK can eliminate intracellular *Listeria* infection in trophoblasts without degranulating or killing the host cells (24). Although ZIKV infects the placenta and fetus and can cause severe birth defects including microcephaly, brain atrophy, and subcortical and chorioretinal and optic nerve atrophy, little is known about the response of decidual immune cells to ZIKV and its effect on maternal–fetal transmission (25).

dNK Kill ZIKV-Infected JEG-3

Although ZIKV infects cultured human fetal trophoblast cell lines grown as single cells or three-dimensional (3D) first-trimester placental cultures, isolated first-trimester primary trophoblast cells (undifferentiated in culture) are difficult to infect without using a very high multiplicity of infection (MOI) (26, 27). To examine the dNK response to ZIKV-infected trophoblasts, we first infected the human trophoblast-like choriocarcinoma cell line JEG-3, whose MHC Class I expression resembles EVT, with the 2015 epidemic PRVABC59 strain of ZIKV. JEG-3 were readily infected (*SI Appendix*, Fig. S1) (26, 28–30). Within 2 d of ZIKV infection with an MOI of 1 to 2, 50 to 70% of JEG-3 became infected and stained with pan-flavivirus envelope antibody. Although the infection was cytopathic at high MOI, only ∼15% of JEG-3 infected at MOI 2 were not viable above background at this time point (*SI Appendix*, Fig. S1 *B* and *C*), making them suitable targets for killing assays. It is worth noting that the PRVABC59 strain and

Significance

Natural killer cells (NK) defend against viruses. Decidual NK (dNK), which comprise ∼70% of decidual leukocytes during early pregnancy, are poorly cytotoxic but promote placentation. Zika virus (ZIKV) can cause fetal loss and birth defects. A strong dNK-mediated antiviral defense could provide a barrier to placental infections. Here, we show that ZIKV infection transforms immune-tolerated trophoblasts into dNK targets because ZIKV replicates in the endoplasmic reticulum (ER) and causes ER stress, which triggers NK killing. Unlike in the case of other viral infections, dNK release their granules and kill ZIKV-infected trophoblasts. In a trophoblast-like cell line, human primary extravillous trophoblasts, 3D villous explants, and *Ifnar1*$^{-/-}$ pregnant mice, dNK reduce placental and fetal viral loads and protect against fetal loss.

Author contributions: S.S.S., A.C.C., S.M., S.B., and J.L. designed research; S.S.S., A.C.C., S.M., and C.O. performed research; S.S.S., A.C.C., S.M., J.L.S., and J.L. analyzed data; and S.S.S., A.C.C., S.M., and J.L. wrote the paper.

Reviewers: M.C., Washington University in St. Louis School of Medicine; and C.B.C., Duke University School of Medicine.

The authors declare no competing interest.

[1]S.S.S., A.C.C., and S.M. contributed equally to this work.

[2]Present address: Department of Pulmonary Immunology, Center for Biomedical Research, The University of Texas Health Science Center at Tyler, Tyler, TX 75708.

[3]To whom correspondence may be addressed. Email: judy.lieberman@childrens.harvard.edu.

This article contains supporting information online at http://www.pnas.org/lookup/suppl/doi:10.1073/pnas.2115410118/-/DCSupplemental.

Published November 16, 2021.

the nonepidemic MR766 strain were not significantly different in JEG-3 cytopathicity (*SI Appendix*, Fig. S1*D*), contrary to what has been described in stem cell-derived trophoblasts (31). dNK isolated from first-trimester healthy human decidua were cocultured with ZIKV-infected JEG-3. Although dNK do not release their cytotoxic granules in response to other viral or *Listeria* infections (19, 24), dNK degranulated against ZIKV-infected JEG-3, assessed by externalization of the internal cytotoxic granule marker CD107a (Fig. 1 *A* and *B*). dNK also killed ZIKV-infected JEG-3 as measured by ^{51}Cr release assay (Fig. 1*C*) and inhibited production of infectious virus, assessed by plaque assay on Vero cells cultured with supernatants from the cocultures (Fig. 1*D*). Cytotoxicity was inhibited by the calcium chelator EGTA, which blocks NK cell degranulation and perforin function (Fig. 1*E*), indicating that killing was mediated by cytotoxic granule release. dNK from multiple human first-trimester samples killed JEG-3 infected with either the 2015 epidemic PRVABC59 or the nonepidemic MR766 strain but did not kill HCMV or HSV-2–infected JEG-3 above background (Fig. 1*F*), even with high infection levels (Fig. 1*G*). A similar level of HCMV infection as achieved in this assay triggers pNK to kill JEG-3 (19). ZIKV is so far the only trophoblast infection known to trigger dNK killing. Killing of JEG-3 infected with the epidemic strain was significantly greater than killing of cells infected with the nonepidemic strain, even though both strains produced statistically similar viral titers (Fig. 1*G*). ZIKV-infected JEG-3 also activated dNK to produce the antiviral and macrophage-activating cytokine IFN-γ (Fig. 1 *H* and *I*). IFN-γ is known to inhibit EVT migration, which is important for placentation (32). Thus ZIKV, unlike other viral infections, turns a trophoblast-like cell line into a dNK target, disrupting tolerance to infected trophoblasts.

ZIKV Down-Regulates HLA-C and HLA-G on JEG-3

Classical MHC Class I molecules strongly inhibit NK activation, but HLA-A and -B are not expressed by EVT (4). Immune tolerance of EVT depends partially on EVT expression of HLA-C, -E, and -G, recognized by the LILRB1, LILRB2, NKG2, and KIR2DL family NK receptors (33). ZIKV and other flaviviruses up-regulate HLA class I in human fibroblasts, endothelial cells, myocytes and neuronal cells secondary to virus-induced type I interferon induction, which inhibits NK killing (34, 35). We verified that ZIKV up-regulates HLA-A/B/C in the U-251 human glioblastoma cell line (*SI Appendix*, Fig. S2 *A* and *B*). Because NK activation depends on expression of HLA and various stress ligands, we examined the effect of PRVABC59 and MR766 infection on JEG-3 expression of HLA and the stress-related NK ligands MICA/B. Neither strain of ZIKV up-regulated HLA-A, -B, -E, or -F or MICA/B on JEG-3 (Fig. 2 *A*–*C*). Both HLA-C and -G were reduced on JEG-3 48 h postinfection with either strain to a similar extent (Fig. 2 *A*–*C*). Consistent with the lack of HLA up-regulation and a previous report (28) ZIKV infection of JEG-3 did not induce *IFNB* or the IFN-stimulated genes, *OAS* and *MX1*, which were up-regulated in U-251 (*SI Appendix*, Fig. S2*C*). In contrast, HSV-2 and HCMV, which cause congenital infection, down-regulated HLA-C but did not affect expression of HLA-G on JEG-3 (Fig. 2 *A*, *D*, and *E*). Notably, ZIKV did

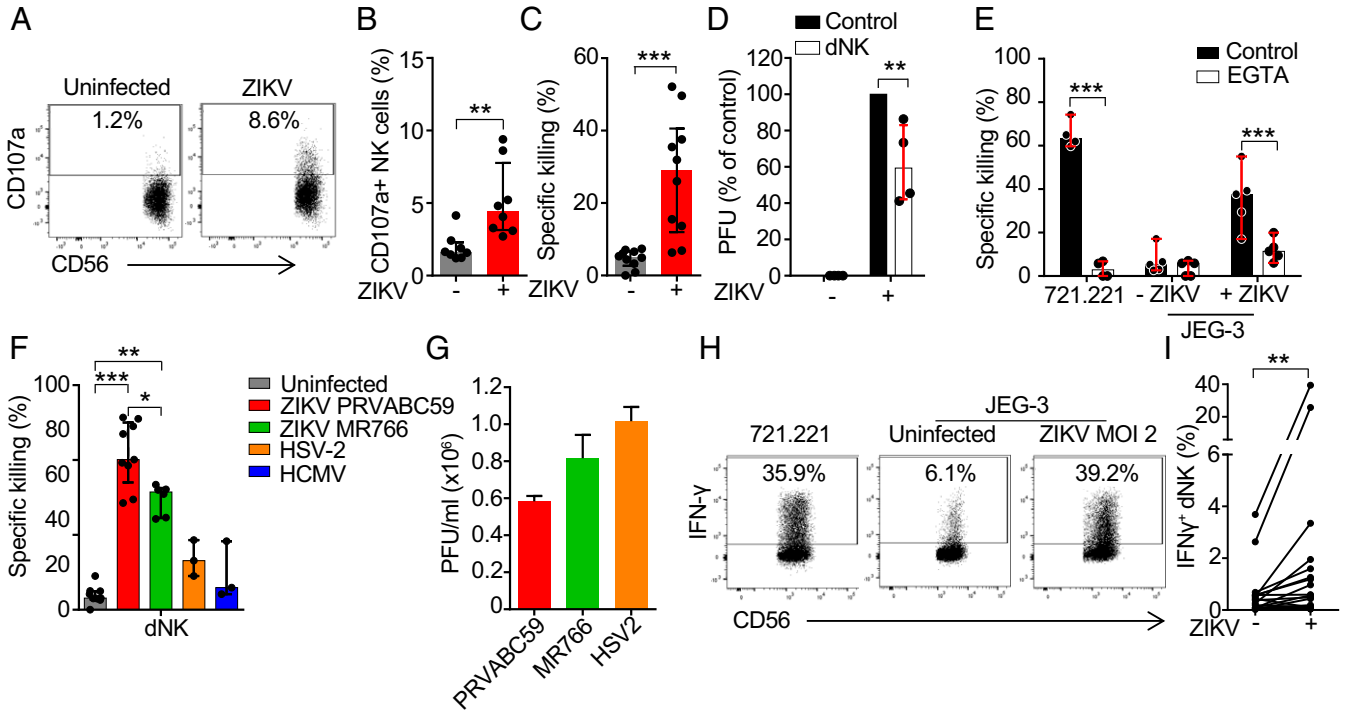

Fig. 1. dNK kill ZIKV-infected JEG-3. (*A* and *B*) Representative flow cytometry plots (*A*) and median proportion (*B*) of dNK degranulating to uninfected and ZIKV PRVABC59–infected JEG-3 (8-h coculture, effector:target [E:T] ratio 1:3) (n = 8). (*C*) dNK specific killing of uninfected and ZIKV PRVABC59–infected JEG-3 (n = 10). (*D*) Viral plaque assay (on Vero cells) of supernatants after 8-h coculture of ZIKV PRVABC59–infected JEG-3 with dNK (E:T ratio 10:1), relative to infected JEG-3 without added NK cells (n = 4). PFU, plaque forming units. (*E*) Effect of EGTA on dNK killing (n = 4). (*F*) Comparison of dNK specific killing of JEG-3 that were uninfected or infected with indicated viruses (n = 3 to 9). (*G*) Levels of infection of the indicated viruses in JEG-3. (*H*) Representative flow cytometry plots of IFN-γ production by dNK after 8-h coculture with 721.221 or uninfected and ZIKV PRVABC59 infected JEG-3 (MOI 2, E:T ratio 1:3) (*I*) and percentage of IFN-γ producing dNK in response to infection (n = 21). Killing assays in *C*, *E*, and *F* were 8-h ^{51}Cr release assays performed at an E:T ratio of 10:1. Bars show median ± interquartile range (*B*–*F*) of biological replicates or mean ± SEM (*G*) of three independent experiments. In all infection experiments, ZIKV (PRVABC59 and MR766), MOI = 2; HSV-2, MOI = 0.5; HCMV, MOI = 3. *P < 0.05; **P < 0.01; ***P < 0.001 by Wilcoxon rank sum test (*B*–*E* and *I*), nonparametric unpaired ANOVA (Kruskal–Wallis test) followed by Dunn's posttest (*F*), and nonparametric paired ANOVA (Friedman's test) followed by Dunn's posttest (*G*).

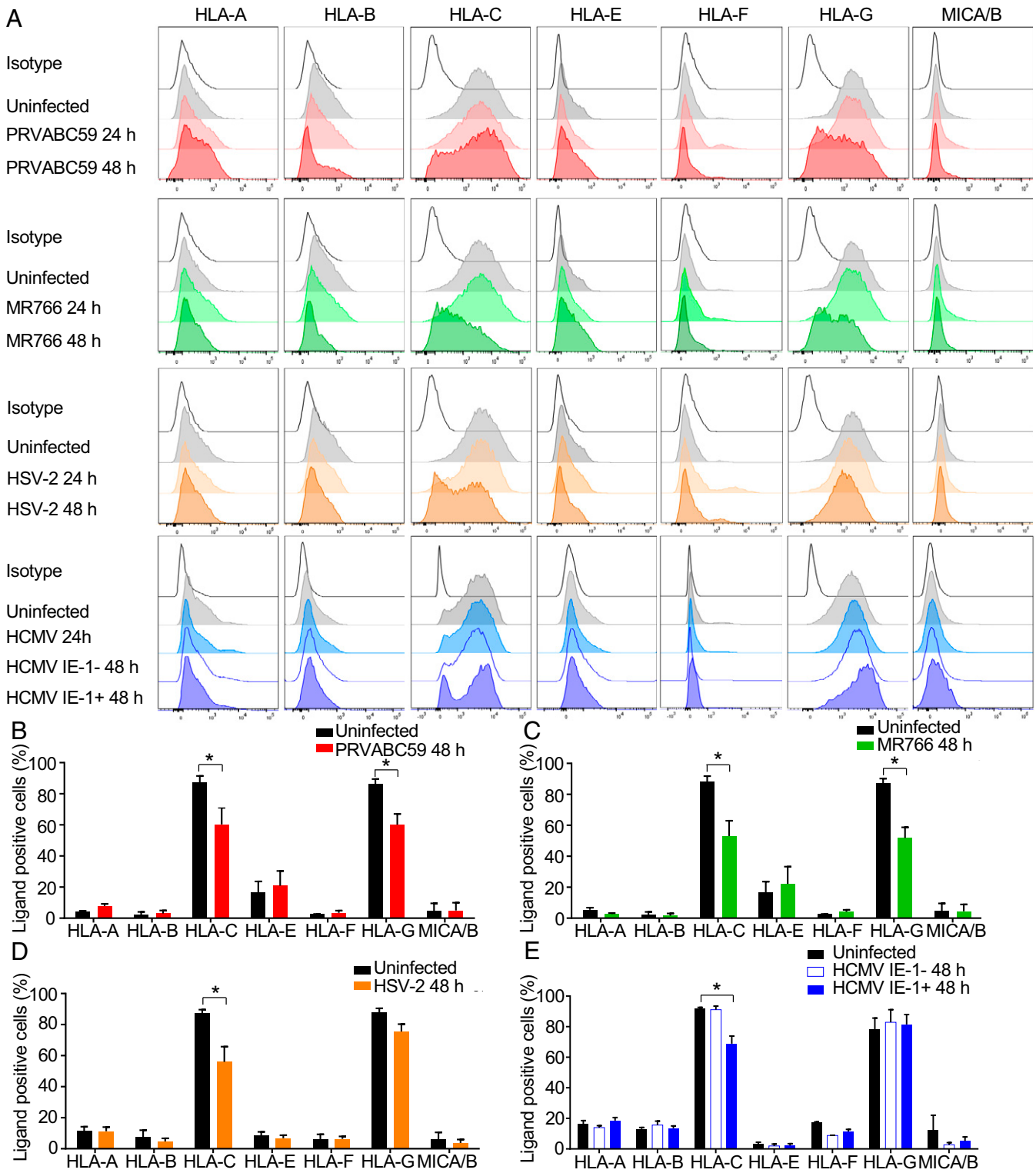

Fig. 2. ZIKV infection down-regulates HLA-C and HLA-G in JEG-3. (*A–E*) Representative flow cytometry plots (*A*) or mean ± SEM values (three to five independent experiments) (*B–E*) of the percentage of HLA and MICA/B positive fractions on uninfected JEG-3 or JEG-3 infected with ZIKV PRVABC59 (MOI 2) (*B*), ZIKV MR766 (MOI 2) (*C*), HSV-2 (MOI 0.5) (*D*), or HCMV (MOI 3) (*E*) for indicated times. IE-1, immediate early protein 1. **P* < 0.05 by Wilcoxon rank sum test (*B–E*).

not reduce *HLA-C* and *HLA-G* messenger RNA (mRNA) in JEG-3 (*SI Appendix*, Fig. S2*D*), suggesting regulation at the protein level. Thus, ZIKV down-regulates HLA-C and -G, which help maintain fetal tolerance, and does not induce other NK-inhibiting classical HLA molecules in JEG-3.

ZIKV Reduces HLA-G Expression in Primary EVT and dNK Eliminate ZIKV-Infected EVT

Next we wanted to verify that ZIKV infects primary human EVT and similarly modifies HLA expression and triggers NK killing of infected cells. Primary placental cells are difficult to

infect in vitro (26), but we were able to infect placental cell suspensions using an extremely high inoculum (10^{12} PFU) (*SI Appendix*, Fig. S3 *A–C*). In these suspensions, ZIKV preferentially infected EVT, identified as B7-H3^{+}CD49e^{+}. On average about 30% of EVT stained for ZIKV E protein, while fewer than 10% of other cells became infected; about half of the infected cells in these cultures were EVT. To study MHC expression and coculture with dNK, we purified EVT (by sorting B7-H3^{+}CD49e^{+} cells) and infected them with the same high MOI of ZIKV PRVABC59, obtaining similar levels of infection as in the full suspension (about 25% on average) (Fig. 3 *A* and *B*). ZIKV significantly down-regulated HLA-C and HLA-G in primary EVT, as we had observed with JEG-3 (Fig. 3 *C* and *D*). When autologous dNK were added to these primary purified cultures for 12 h, the percentage of infected EVT decreased significantly on average by about one-half, but dNK effectiveness varied among donors (Fig. 3 *A* and *B*). Thus, ZIKV infects primary trophoblasts and causes HLA-G and -C down-regulation, and infection is reduced by dNK.

To verify that the results obtained with primary EVT and JEG-3 apply to intact placental tissue, 3D placental explants (which survive up to 6 d; *SI Appendix*, Fig. S3*D*) were infected with a high viral inoculum (10^{8} PFU) for 72 h (Fig. 3 *E–G*) (1, 36, 37). Infection, detected by staining for envelope E protein, incorporated into mature virions, and NS2B protease, expressed during viral replication, was prominent in CD49a^{+}CDH-1^{+} cells with large nuclei located at the tips of the villi, which identified them as EVTs (~47% of the infected cells) and in cytotrophoblasts (~35% of the infected cells; CTs, identified as cells with small nuclei located under EVTs or syncytium, expressing CDH-1) (Fig. 3 *E* and *F*). ZIKV was virtually undetected in stromal cells and syncytiotrophoblasts (STs; identified as SDC-1^{+} cells with small nuclei in a continuous layer surrounding the villi). Indeed, STs have been shown to resist ZIKV infection, although ZIKV can alter the permeability of the syncytium leading to infection of mesenchymal cells in the chorionic villi (38). Coculture of infected explants with autologous dNK significantly reduced the number of infected EVT by about half, indicating that dNK can help control ZIKV infection in tissue (Fig. 3*G*).

ZIKV-Induced Endoplasmic Reticulum Stress Down-Regulates HLA-C and -G and Is Critical for NK Killing

HLA expression, which plays a critical role in NK activation, is reduced by endoplasmic reticulum (ER) stress (39, 40). Because ZIKV replicates in the ER and is known to cause ER stress (41, 42), we hypothesized that ER stress induced by ZIKV was responsible for HLA-C and -G down-regulation in infected JEG-3 and primary trophoblasts, which would explain lower protein levels without a decrease in mRNA. ZIKV infection induced ER stress in JEG-3 to a similar extent as the ER stressor tunicamycin (which induces the unfolded protein response [UPR] by blocking N-linked glycosylation) (43), as assessed by increased *XBP1* splicing and induction of ER stress-related mRNAs, *BIP*, *CHOP*, *ATF4*, and *GRP94* (30) (Fig. 4*A*). To determine whether ZIKV also causes ER stress in vivo, we measured *Xbp1* splicing, *Chop* and *Bip* expression by qRT-PCR in total placental RNA isolated on embryonic day (E)15.5 from *Ifnar*$^{-/-}$ (A129) mice that were uninfected or infected with ZIKV on E6.5 (Fig. 4*B*). Indeed, ZIKV infection caused significant ER stress in the placenta. Thus, ZIKV infection causes ER stress in vitro in a human trophoblast-like cell line and in the placentas of *Ifnar*$^{-/-}$ mice infected early in pregnancy.

To identify the ZIKV components that induce ER stress we used a reporter assay to quantify *XBP1* splicing and the amount of active ATF6 transcription factor in JEG-3 cotransfected with either pFLAG-XBP1u-Fluc or p5xATF6-GL3 + pRLSV40P reporter and plasmids encoding individual ZIKV proteins (*SI Appendix*, Fig. S4 *A* and *B*). Overexpression of seven ZIKV proteins, the glycoproteins prM-E, E, and NS1 and the ER membrane-anchored small hydrophobic proteins NS2A, NS2B, and (2K)-NS4B, increased luciferase activity, while expression of six genes that encode for C, M, NS2B, N3, NS4A, and NS5 did not (*SI Appendix*, Fig. S4*B*). By and large, the ZIKV proteins that project into the ER lumen in the initially synthesized ZIKV polyprotein triggered ER stress, while the proteins that project into the cytosol did not. NS2B-3, encoding for a fusion of the NS3 protease and its cofactor NS2B, induced higher reporter expression than NS2B or NS3 alone. Not surprisingly, overexpression of most ZIKV genes that caused *XBP1* splicing or ATF6 activation also partially down-regulated HLA-C/G (*SI Appendix*, Fig. S4 *C* and *D*).

To determine if ER stress alone makes JEG-3 susceptible to dNK killing, JEG-3 were treated with tunicamycin for 24 h using a concentration that causes ER stress without apoptosis (Fig. 4*A*). Tunicamycin down-regulated both HLA-C and -G in JEG-3 and led to dNK killing (Fig. 4 *C* and *D*). The ER stress inhibitor salubrinal, which prevents dephosphorylation of the eukaryotic translation initiation factor 2 alpha (eIF2α) (44), inhibited both ZIKV- and tunicamycin-induced *XBP1* splicing and induction of ER stress signature genes (Fig. 4*A*). Moreover, salubrinal also restored HLA-C/G expression in ZIKV-infected JEG-3 (Fig. 4 *E* and *F*) and inhibited dNK killing of tunicamycin-treated and ZIKV-infected JEG-3 (Fig. 4 *D* and *G*). Thus, ER stress in a ZIKV-infected trophoblast cell line causes HLA-C/-G down-regulation.

The NK Activating Receptor NKp46 that Recognizes ER-Stressed Cells Contributes to dNK Killing of ZIKV-Infected JEG-3

NK killing requires activating receptor ligation by target cells. We recently found that the NKp46 activating receptor, ubiquitously expressed on NK and also on some innate lymphoid cells, recognizes ER-stressed target cells by binding to calreticulin (CRT), an ER-resident protein that is externalized and presented on the cell membrane during ER stress (45). Moreover, we also showed that ZIKV-induced ER stress up-regulates CRT on JEG-3, increases pNK binding to infected cells, and triggers their killing of ZIKV-infected JEG-3. pNK killing is inhibited by antibodies to CRT or NKp46 or by knocking down or knocking out their genes, *CALR* or *NCR1*. Because dNK are less cytotoxic than pNK we first examined which activating receptors are expressed on dNK (Fig. 4*H*). dNK strongly expressed NKp46 and NKp30 and weakly expressed NKG2D and 2B4, but much less than pNK. dNK expression of NKp44, NKp80, NKG2C, or DNAM-1 was not detected. NKp46 blocking antibody, but not anti-NKp30, significantly inhibited dNK killing of ZIKV-infected JEG-3, suggesting that NKp46 on dNK is an activating receptor triggered by ZIKV infection, as previously found for pNK (45) (Fig. 4*I*). Taken together, these data show that ZIKV-induced ER stress down-regulates HLA-C and -G, ligands for dNK inhibitory receptors, and increases activation of NKp46 to disrupt the balance of NK activating and inhibitory receptor binding at the trophoblast cell surface, triggering dNK killing of ZIKV-infected trophoblasts.

NK Depletion in Pregnancy Aggravates ZIKV Infection in A129 Mice

To promote infection, ZIKV dampens but does not eliminate (35) the induction of type-I IFNs in human cells but is less able to do this in mouse cells (46). As a consequence, wild-type (WT) mice are difficult to infect with ZIKV, and A129 mice, deficient in the Type I IFN receptor gene *Ifnar*, are used for

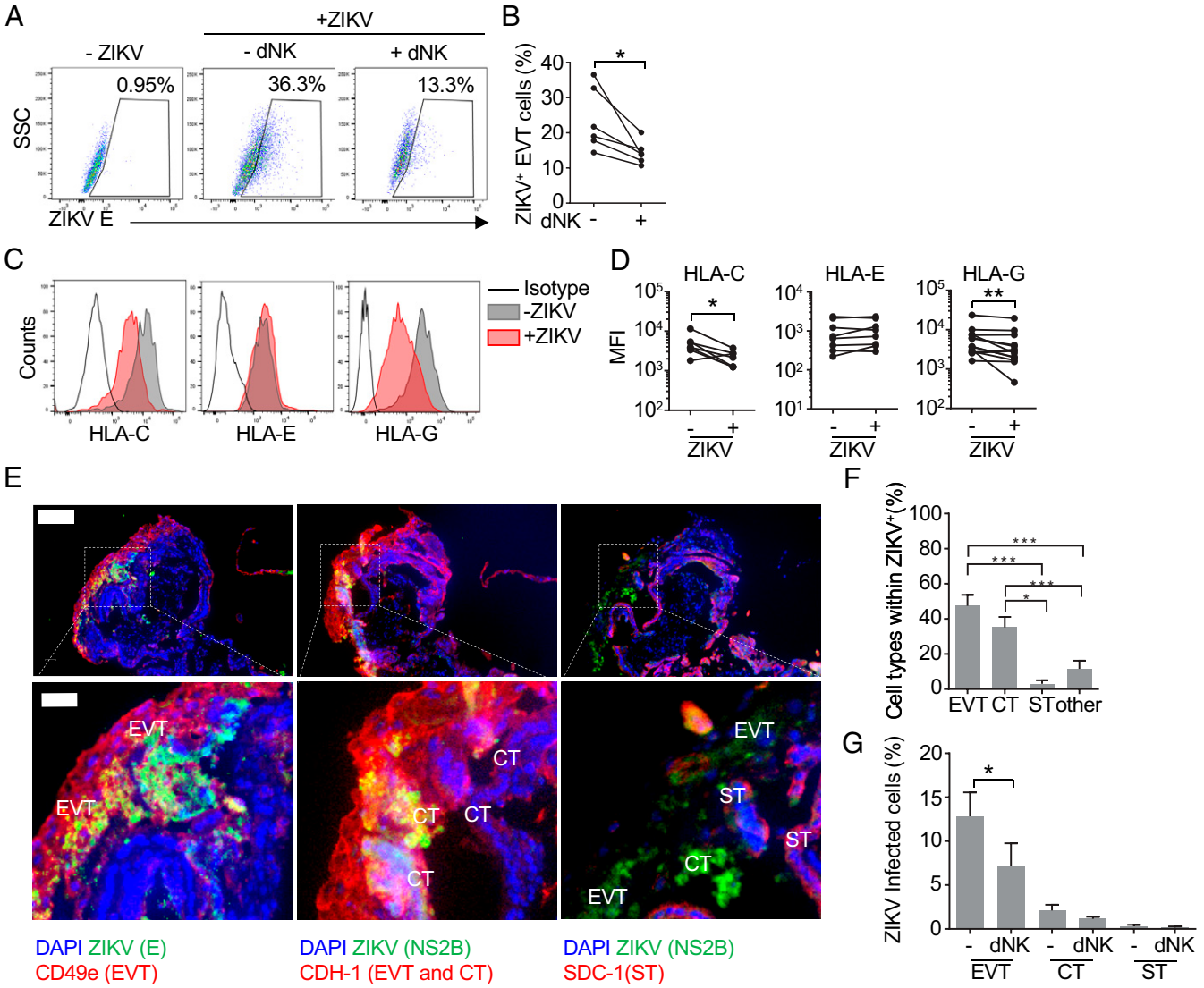

Fig. 3. ZIKV mostly infects extravillous and cytotrophoblasts in placental explants and down-regulates HLA-G and HLA-C in isolated EVT. (*A*) Representative flow cytometry dot plots of intracellular staining for ZIKV protein E in purified primary EVT that were uninfected (*Left*) or infected with ZIKV (10^{12} PFU) and cultured alone for 36 h (*Middle*) or alone for 24 h followed by 12-h coculture with autologous dNK (E:T ratio 10:1) (*Right*). (*B*) Percentage of ZIKV$^+$ cells in purified infected EVT cultures that were cocultured or not with a 10-fold excess of autologous dNK ($n = 6$) for 12 h (after 24-h infection). (*C*) Representative flow cytometry histograms of HLA-C (*Left*), HLA-E (*Middle*), and HLA-G (*Right*) surface expression in uninfected and ZIKV-infected (24 h, 10^{12} PFU) isolated purified EVT. (*D*) Mean fluorescence intensity (MFI) of HLA-C (*Left*), HLA-E (*Middle*), and HLA-G (*Right*) in uninfected or ZIKV-infected purified EVT ($n = 7$ to 13). (*E*) Representative immunofluorescence images of three consecutive 5-μm cryosections of a placental villous tree infected with ZIKV-PRVABC59 for 72 h (10^8 PFU) and stained for DAPI, ZIKV proteins (NS2B and E), integrin-α5/CD49a (EVT marker), E-cadherin (CDH-1, cytotrophoblast [CT] and EVT marker), and SDC-1 (syncytiotrophoblast [ST] marker). Cell types were identified by surface marker staining, nuclear size, and localization in tissue. (Scale bar, 100 μm [insets in the bottom, 25 μm].) (*F*) Distribution of ZIKV-infected placental cell types 72 h after infection of 3D villous explants. Bars represent the mean ± SEM of the percentages calculated in 10 to 15 imaging fields (217× magnification) from three donors. (*G*) Percentage of EVT, CT, and ST infected with ZIKV in the presence or absence of autologous dNK. Bars represent the mean ± SEM of the percentages calculated in 10 to 15 imaging fields (217× magnification) from three donors. *$P < 0.05$; **$P < 0.01$; ***$P < 0.001$ by Wilcoxon rank sum test (*B* and *D*), paired nonparametric ANOVA (Friedman's test) followed by Dunn's posttest comparing each cell type to each other (*F*), and Kolmogorov–Smirnov test (*G*).

infection studies (47). Type I IFNs have been implicated as mediators of pregnancy complications during ZIKV infection in mice (48). To assess the cellular immune response to ZIKV early in pregnancy, pregnant A129 or WT mice were infected with 10^3 PFU PRVABC59 strain intraperitoneally on E6.5 (equivalent to the human first trimester). Some mice were depleted of NK, CD8 T cells, or B cells before ZIKV challenge, using cell-type-specific antibodies (anti-asialo GM1 glycoprotein, anti-CD8, and anti-CD20, respectively) administered before and after infection and control mice were treated with anti-KLH rat IgG2b control antibody. Selective depletion of each cell type was verified by examining maternal blood lymphocytes the day before infection (*SI Appendix*, Fig. S5*A*). Although anti-asialo GM1 depletes both basophils and NK, basophils are not known to play a role in ZIKV pathogenesis. None of the WT mice became infected. Fifteen of 16 A129 mice infected with this low inoculum and treated with the control antibody carried their pregnancies to E15.5, when mice were killed (Fig. 5*A*). The number of viable fetuses on E15.5 in infected A129 mice was not statistically different from that in uninfected mice and antibody depletion did not significantly affect the litter size, but fetal weights were significantly reduced by infection and did not change with antibody

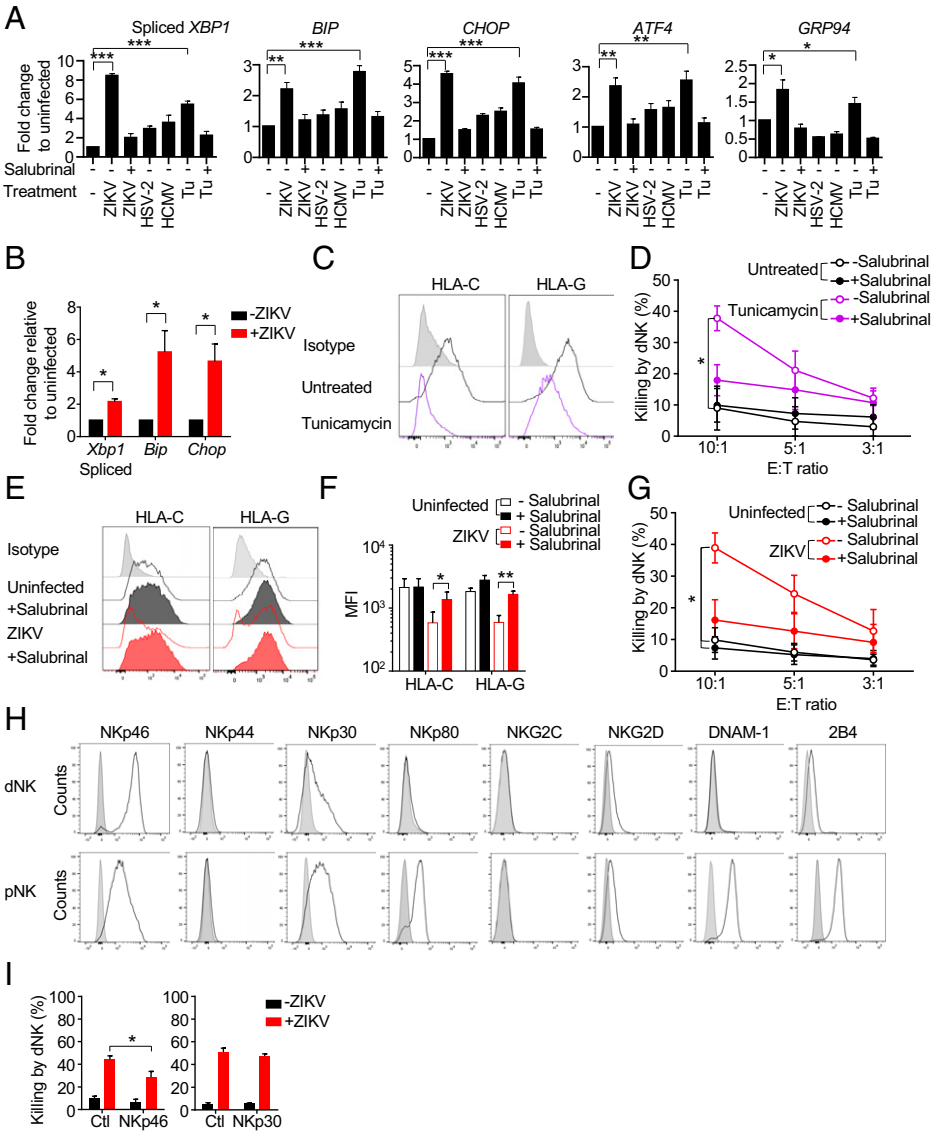

Fig. 4. ZIKV-induced ER stress mediates HLA-C and -G down-regulation and NK killing. (*A*) ER stress, assessed by *XBP1* splicing and increases in *BIP*, *CHOP*, *ATF4*, and *GRP94* mRNA in JEG-3 that were uninfected or infected with ZIKV PRVABC59, HSV-2, or HCMV for 1 to 2 d or treated with tunicamycin (Tu) for 1 d. Some samples were pretreated with the ER stress inhibitor salubrinal as indicated. mRNA levels, determined by qRT-PCR, were normalized to *ACTB* ($n = 3$ independent experiments). (*B*) Assessment of ER stress in total mRNA harvested from E15.5 placentas of pregnant *Ifnar1*$^{-/-}$ dams that were uninfected or ZIKV-infected with ZIKV PRVABC59 on E6.5 ($n = 4$). mRNAs were measured by qRT-PCR, normalized to *Actb*, and shown relative to uninfected mouse placentas. (*C*) Representative flow cytometry histograms of the effect of 24-h tunicamycin treatment on the expression of HLA-C and –G in JEG-3. (*D*) Specific dNK killing (8-h Cr release assay) of JEG-3 that were treated or not with tunicamycin for 24 h in the presence or absence of salubrinal ($n = 3$). (*E*) Representative flow cytometry histograms and (*F*) mean fluorescence intensity (MFI) of HLA-C and HLA-G expression in uninfected or ZIKV PRVABC59–infected JEG-3 that had been pretreated or not with salubrinal ($n = 3$ independent experiments). (*G*) Specific dNK killing (8-h Cr release assay) of uninfected and ZIKV PRVABC59–infected JEG-3 that had been pretreated or not with salubrinal ($n = 5$). (*H*) Representative flow cytometry histograms of expression of activating receptors in freshly isolated dNK and pNK. (*I*) Effect of blocking antibodies for the indicated receptors on dNK killing of uninfected (black) or ZIKV-infected (red) JEG3 (8-h Cr release, E:T ratio 10:1) ($n = 3$ to 9). Ctl, control antibody. Bars represent mean ± SEM. In all infection experiments, ZIKV (PRVABC59 and MR766), MOI = 2; HSV-2, MOI = 0.5; and HCMV, MOI = 3. *$P < 0.05$; **$P < 0.01$; ***$P < 0.001$ by unpaired one-way ANOVA (*A*), unpaired *t* test (*B* and *F*), nonparametric paired ANOVA (Friedman's test followed by Dunn's posttest) of areas under curves (*D* and *G*), and Wilcoxon rank sum test (*I*).

depletion ($n = 35$ per group, $P = 0.02$) (Fig. 5 *B* and *C*). All of the A129 mice and their fetuses became infected as assessed by qRT-PCR of maternal blood and spleen, placentas, and fetal heads on E15.5 (Fig. 5 *D*–*G*). Depletion of NK or CD8 T cells, but not B cells, increased viral loads in both the tissues of dam and fetus 9 d postinfection (Fig. 5 *D*–*G*). The proportion of dams with failed pregnancies was significantly higher in NK- and CD8 T cell-depleted mice, but B cell depletion had no significant effect on pregnancy outcome (Fig. 5*A*). However, depletion of NK or CD8 T cells did not affect fetal weights or litter size of surviving pregnancies, when compared to control antibody treated infected animals. Taken together these data indicate that on balance NK and CD8 T cells protect the fetus from ZIKV infection early in pregnancy in mice. Although ZIKV antibodies and vaccination strategies designed to induce ZIKV antibodies very effectively protect mice from ZIKV transmission (49), and transplacental antibody transfer from ZIKV-infected mothers to fetus has been reported (50), depleting B cells likely had no effect in this model because the native antibody response does not develop until weeks after viral exposure, while the NK response is immediate

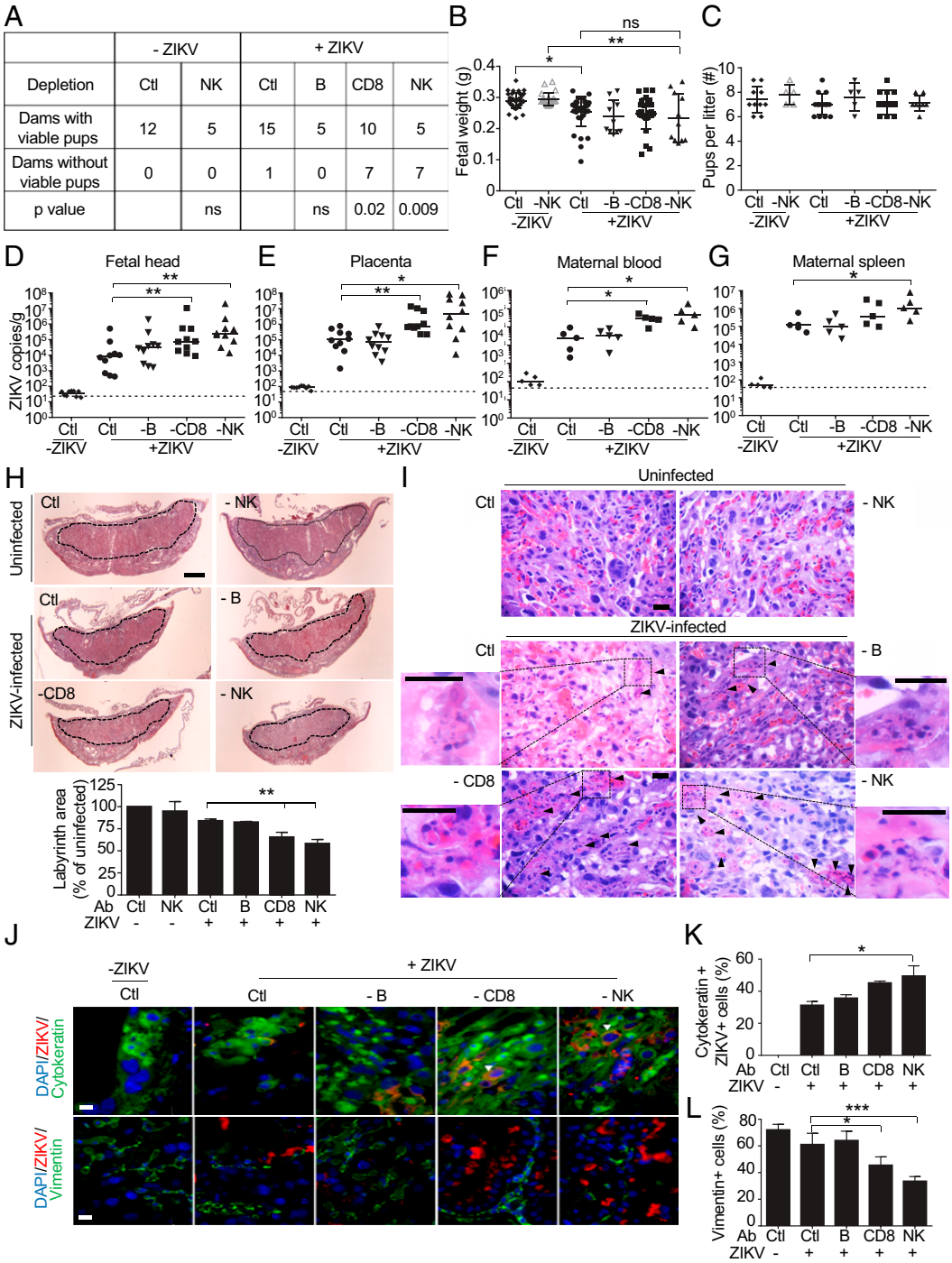

	- ZIKV		+ ZIKV			
Depletion	Ctl	NK	Ctl	B	CD8	NK
Dams with viable pups	12	5	15	5	10	5
Dams without viable pups	0	0	1	0	7	7
p value		ns		ns	0.02	0.009

Fig. 5. NK or CD8 T cell depletion compromises pregnancy after ZIKV PRVABC59 infection of A129 mice. (*A*) Pregnancy outcome of uninfected and ZIKV PRVABC59–infected (10^3 PFU on E6.5) *Ifnar1*$^{-/-}$ dams, treated with control antibody or depleted of B cells, CD8, or NK cells before and after infection (*P* values by χ^2-square test comparing specific depletion with control [Ctl] antibody). (*B* and *C*) Fetal weight (*B*) (n = 11 to 36) and number of pups/litter (*C*) (n = 5 to 15) on E15.5. (*D*–*G*) Viral burden (by qRT-PCR relative to *Actb*) on E15.5 in fetal head (*D*) (n = 10), placenta (*E*) (n = 10), and maternal serum (*F*) (n = 5) and spleen (*G*) (n = 5) of the same dams. Data represent individual mice, pooled from two or three independent experiments. Dotted lines represent the limit of sensitivity of the assay. (*H*) Representative hematoxylin and eosin staining of mouse placentas on E15.5 from mice treated with control (Ctl) or depleting antibodies (*Top*, labyrinth marked by dotted line; scale bar, 1 mm) and mean labyrinth cross-sectional area compared to uninfected control mice given Ctl antibody (Ab) (*Bottom*) (n = 3). (*I*) Representative hematoxylin and eosin–stained mouse placental sections from uninfected and ZIKV-infected dams treated with control or indicated depleting antibody on E15.5. Arrows indicate apoptotic cells and insets display magnified images of the indicated area. (Scale bar, 10 μm.) (*J*) Representative immunofluorescence microscopy images of placentas from uninfected or ZIKV-infected pregnant dams treated with Ctl or depleting antibody and stained for cytokeratin (CK, trophoblast marker) or vimentin (V, endothelial/stromal cell marker) and ZIKV proteins (mouse serum against ZIKV) and DAPI. Infected giant trophoblasts are indicated by arrows. (Scale bars, 10 μm.) (*K*) Mean percentage of CK+ cells that stain for ZIKV in placentas from uninfected or ZIKV-infected pregnant dams treated with control or depleting Ab (n = 4 or 5 mice per group). (*L*) Percentage of V+ cells per high-power field in infected placentas compared to placentas from uninfected mice treated with Ctl Ab (n = 4 or 5 mice per group). Bar graphs show mean ± SEM. $^*P < 0.05$; $^{**}P < 0.01$; $^{***}P < 0.001$ (*B*, *C*, *H*, *K*, and *L*) by ordinary one-way ANOVA followed by Tukey's multiple comparison test and (*D*–*G*) by Mann–Whitney *U* test. ns, not statistically significant.

and the CD8 T cell response to viruses begins to be detected within 5 to 7 d.

To understand how ZIKV causes fetal loss and such significant intrauterine growth restriction (IUGR), we compared the histology of E15.5 placentas of mice that were infected with ZIKV on E6.5 with uninfected mice and also examined the effect of depletion of B, CD8 T, and NK cells on viral load and placental pathology. The labyrinth is the part of the placental disk that contains the villi, which transfer nutrients from the maternal blood to the fetus. Placental viral loads increased significantly with NK ($n = 10$, $P = 0.01$) or CD8 T cell depletion ($n = 10$, $P = 0.003$) but not B cell depletion (Fig. 5*E*). The labyrinth area of infected mice given control antibodies was also reduced compared to uninfected control mice and was further significantly reduced in NK- and CD8 T cell-depleted mice ($n = 5$, $P = 0.009$ for CD8; $n = 5$, $P = 0.008$ for NK depletion) (Fig. 5*H*). Of note, NK depletion did not affect labyrinth size in uninfected mice, so the effect of NK cell depletion was due to ZIKV infection. The placentas of infected mice showed severe pathology, with trophoblast apoptosis and fetal red blood cell karyorrhexis, which were exacerbated in mice depleted of NK cells (Fig. 5*I*). In placentas costained for ZIKV (using ZIKV mouse antiserum) and trophoblast CK (cytokeratin) or stromal and endothelial cell V (vimentin) markers, ZIKV infection was detected in about a third of CK+ trophoblasts and was rare in V+ cells (Fig. 5*J*). Moreover, infection significantly increased in NK-depleted mice so that about half of CK+ cells stained for ZIKV ($n = 5$, six fields per sample, $P = 0.02$ for NK depletion relative to control antibody) (Fig. 5*K*). The placentas of NK and CD8-depleted animals also had reduced endothelial cell numbers (Fig. 5*L*). Thus, although uterine NK (uNK) could potentially contribute to fetal pathology by killing infected trophoblasts, the depletion experiments on balance indicate that CD8 T and NK cells protected against ZIKV infection in pregnant mice since spontaneous abortions, viral loads and placental pathology increased and labyrinth size decreased with CD8 T or NK cell depletion.

Discussion

Here we show that ZIKV is unique among congenital infections because it triggers dNK to degranulate and kill infected trophoblast-like cells, breaking tolerance of infected placental cells. ZIKV infection of a trophoblast-like cell line and of isolated primary human trophoblasts from normal human first-trimester pregnancies down-regulated HLA-G, a nonclassical HLA molecule that plays an important role in immune tolerance by binding to NK switch-motif receptors (51). HLA-G and -C down-regulation was linked to ZIKV replication in the ER, which causes secondary ER stress. An ER stress inhibitor, salubrinal, both blocked HLA-G and -C down-regulation and inhibited dNK killing of ZIKV-infected trophoblast-like cells. Although we did not evaluate other flaviviruses in this study, since they rarely cause congenital infections, they also replicate in the ER and likely also induce ER stress (52), perturb classical and nonclassical HLA expression, and turn infected cells into NK targets. Mice infected with ZIKV early in pregnancy also showed evidence of placental ER stress. IUGR was the most salient pathology in ZIKV-infected mice.

It is worth noting that ER stress and the UPR are hallmarks of IUGR and the closely associated preeclampsia syndrome, as well as microcephaly (53–59). A recent report using cerebral organoids further identified an UPR signature during microcephaly pathogenesis (60). Our results showing induction of ER stress and up-regulation of an UPR signature in ZIKV-infected placentas suggest that ZIKV-induced ER stress may be a root cause of birth defects (61, 62). ZIKV infection also leads to metabolic alterations, mitochondrial dysfunction, and inflammation in placental cells and these changes contribute to tissue damage in the placenta (63–65). Placental cells constitutively secrete interleukin (IL)-1β, indicative of inflammasome activation (66), and express high levels of gasdermin E, which may contribute to IL-1β release (12). ZIKV exacerbates this inflammatory state (67, 68). Indeed, blocking IL-1 signaling with an IL-1 receptor agonist in ZIKV-infected pregnant dams improves placental function, increases fetal viability and reduces birth defects in mice (69). ZIKV-induced ER stress could contribute to metabolic alterations in the placenta that lead to placental inflammation and tissue damage.

A previous in vitro study suggested that pNK do not kill ZIKV-infected primary human cells because ZIKV induces type I IFNs, which up-regulate classical HLA molecules that inhibit NK killing (35). However, pNK from ZIKV-infected patients show signs of activation (70) and murine pNK that developed memory-like characteristics after in vivo ZIKV infection exhibited superior antiviral capacity (71). In the present study, we confirmed that ZIKV up-regulates type I IFNs in a neuronal cell line but found that ZIKV doesn't induce type I IFNs and inhibits classical HLA expression and MICA/B stress signals in a human trophoblast cell line. Thus, in trophoblasts, ER stress, rather than IFN induction, regulates changes in HLA expression and causes down-regulation, while in other cells, especially neurons, ZIKV induces Type I IFNs that up-regulate HLA. These differences in HLA expression help make trophoblasts good NK targets but may inhibit NK recognition and control of infection in the brain and elsewhere.

NK killing generally requires activation of an NK activating receptor in addition to lack of inhibitor receptor signaling. We recently found that an activating receptor, NKp46, expressed ubiquitously on pNK and dNK, selectively recognizes ZIKV-infected JEG-3 (45). ZIKV induction of ER stress is recognized by NKp46 in trophoblasts and probably also in other cells. It will be worthwhile to examine in detail how dNK and pNK activating and inhibitory receptors respond to different cell types infected with ZIKV and how the effects of ZIKV infection and ER stress are integrated and sensed by NK to result in either tolerance or killing and cytokine release. Another NK activating receptor, that might be induced in dNK during placental ZIKV infection, could also be triggered by ZIKV-infected trophoblasts, since inhibition of dNK killing of ZIKV-infected JEG-3 was only partially blocked by anti-NKp46 (Fig. 4*I*). It is likely that this early innate immune NK response will have a profound effect on disease course. The variability we noted among human samples in dNK degranulation, killing and IFN-γ response to ZIKV-infected JEG-3 and primary trophoblasts suggests that there may be genetic or nongenetic factors that influence NK responses and the consequences of infection.

The protective versus pathological role of dNK that kill ZIKV-infected trophoblasts is difficult to predict ab initio. On the one hand, dNK help control viral replication and spreading by killing infected cells. On the other, tolerance to infected placental cells is broken and trophoblasts, which play a critical role in placentation, are likely destroyed by both viral cytopathicity and dNK killing. Moreover, dNK respond to ZIKV-infected JEG-3 by producing IFN-γ, which can inhibit EVT invasion of the decidua, a key mediator of vascular remodeling in the placenta (32). Here we found that depletion of either CD8 T cells or NK prior to a low inoculum of ZIKV early in pregnancy in *Ifnar1*$^{-/-}$ mice worsened viral loads in the fetus, placenta, and mother and led to spontaneous abortions, which were rare in control antibody-treated mice challenged with this viral inoculum. Thus, innate and adaptive killer lymphocytes on balance protect against ZIKV infection in pregnancy. In particular, despite disruption of tolerance and the importance of dNK in regulating trophoblast migration, maturation, and placentation, IUGR secondary to infection, assessed by fetal weights and

placental size, was worsened by uNK depletion. Thus, ZIKV infection in the absence of antiviral killer lymphocytes is likely overall more cytopathic for the placenta since dNK lysis of infected EVT likely limits the spread of infection to uninfected trophoblasts, reducing, but not eliminating, the pathological consequences. NK depletion in the absence of ZIKV had no apparent effect on placental development, as assessed by labyrinth size, unlike IL15-deficient mice that lack NK cells and have smaller placentas (72). This suggests that other IL15-responsive cell types besides NK cells, such as macrophages, might be important contributors to placental development (73). The effect of CD8 T cell depletion on ZIKV infection in pregnancy was previously shown (74, 75). Protection by CD8 T cells was likely due to peripheral CD8 T cell control of viral replication, since CD8 T cells are strongly activated by ZIKV infection in the periphery (76–79) and are mostly absent in the placenta early in pregnancy in both mice and humans (79, 80). T cells constituted only a few percent of decidual hematopoietic cells and did not increase with ZIKV infection compared to uninfected mice until very late in pregnancy. Since ZIKV increases MHC expression in cells other than trophoblasts (35), which is predicted to dampen NK reactivity, the major effect of NK depletion in pregnancy may be largely secondary to uNK activity locally in the decidua. However, there is no way to selectively deplete uNK without depleting pNK, so our depletion experiment could not separate the importance of local placental NK from systemic NK in the better outcome of ZIKV infection in NK-competent mice.

Why the Brazilian epidemic strain of ZIKV is so virulent, especially in pregnancy, is not well understood. The epidemic strain differs from the prior strain by only 13 amino acids and an insertion in the 3' untranslated region stem loop (81). Mutations that increase virulence are concentrated in PrM and the envelope regions of the virus (81, 82). These proteins contribute to ZIKV ER stress in our study. The epidemic and nonepidemic strains did not differ in JEG-3 cytopathicity in our study, but dNK killed JEG-3 infected with the epidemic strain significantly more than the nonvirulent strain. Studies to compare infection of villous explants with different strains in the presence of dNK could examine whether the epidemic strain causes more placental pathology.

In conclusion, congenital ZIKV infection induces ER stress that activates dNK and antiviral control in placental trophoblasts. This dNK defense is relevant in vivo since NK depletion worsened congenital ZIKV disease. Previously, dNK have not been thought to have a role in controlling placental infection. We recently demonstrated an antimicrobial role for dNK in placental *Listeria monocytogenes* infection (24) and decidual HCMV infection (19, 83). These results and this study suggest that dNK help control placental infection to protect the fetus.

Materials and Methods

JEG-3 was infected with ZIKV PRVABC59 or MR766, HSV-2 or HCMV or treated with tunicamycin. Human placental villi and purified cells were isolated from discarded, deidentified healthy human placental and decidual tissue (gestational age 6 to 12 wk) with approval from Harvard and Boston Children's Hospital Human Institutional Review Committees and infected with ZIKV. Pregnant *Ifnar1*$^{-/-}$ and WT C57BL/6 mice were intraperitoneally infected with ZIKV PRVABC59 on E6.5 and killed at E15.5 to assess pregnancy loss and viral loads in mother, placenta, and fetus by plaque assay. Mouse studies were approved by the Harvard Medical School Institutional Animal Care and Use Committee. All relevant materials and methods, including isolation and culture of human placental tissue, cells and cell lines, viruses, infection protocols, assays of NK function, flow cytometry and confocal microscopy, mouse experimental protocols and analysis of placental histology, and statistical methods are described in *SI Appendix, Materials and Methods*.

Data Availability. Constructed plasmids have been deposited at Addgene (https://www.addgene.org/Judy_Lieberman/). All other study data are included in the article and/or *SI Appendix*.

ACKNOWLEDGMENTS. This work was supported by NIH Grants HD87689 and AI45862 to J.L.S. and J.L., a Jeffrey Modell Foundation fellowship to S.S.S., and an NIH T32 fellowship to S.M. We thank Don Coen (Harvard Medical School) for HCMV-IE-1-GFP, Mary Carrington (National Cancer Institute) for HLA-C antibody, and R. Bronson (Harvard Medical School) for technical help.

1. T. Tabata *et al.*, Zika virus targets different primary human placental cells, suggesting two routes for vertical transmission. *Cell Host Microbe* **20**, 155–166 (2016).
2. J. J. Miner, M. S. Diamond, Zika virus pathogenesis and tissue tropism. *Cell Host Microbe* **21**, 134–142 (2017).
3. L. J. Yockey *et al.*, Vaginal exposure to Zika virus during pregnancy leads to fetal brain infection. *Cell* **166**, 1247–1256.e4 (2016).
4. R. Apps *et al.*, Human leucocyte antigen (HLA) expression of primary trophoblast cells and placental cell lines, determined using single antigen beads to characterize allotype specificities of anti-HLA antibodies. *Immunology* **127**, 26–39 (2009).
5. R. Apps, L. Gardner, A. Moffett, A critical look at HLA-G. *Trends Immunol.* **29**, 313–321 (2008).
6. T. Tilburgs *et al.*, Human HLA-G+ extravillous trophoblasts: Immune-activating cells that interact with decidual leukocytes. *Proc. Natl. Acad. Sci. U.S.A.* **112**, 7219–7224 (2015).
7. A. Moffett, C. Loke, Immunology of placentation in eutherian mammals. *Nat. Rev. Immunol.* **6**, 584–594 (2006).
8. A. Erlebacher, Immunology of the maternal-fetal interface. *Annu. Rev. Immunol.* **31**, 387–411 (2013).
9. J. Hanna *et al.*, Decidual NK cells regulate key developmental processes at the human fetal-maternal interface. *Nat. Med.* **12**, 1065–1074 (2006).
10. J. M. Monk, S. Leonard, B. A. McBey, B. A. Croy, Induction of murine spiral artery modification by recombinant human interferon-gamma. *Placenta* **26**, 835–838 (2005).
11. B. A. Croy *et al.*, Uterine natural killer cells: Insights into their cellular and molecular biology from mouse modelling. *Reproduction* **126**, 149–160 (2003).
12. R. Vento-Tormo *et al.*, Single-cell reconstruction of the early maternal-fetal interface in humans. *Nature* **563**, 347–353 (2018).
13. M. M. Faas, P. de Vos, Uterine NK cells and macrophages in pregnancy. *Placenta* **56**, 44–52 (2017).
14. J. R. Robbins, A. I. Bakardjiev, Pathogens and the placental fortress. *Curr. Opin. Microbiol.* **15**, 36–43 (2012).
15. M. B. Vigliani, A. I. Bakardjiev, Intracellular organisms as placental invaders. *Fetal Matern. Med. Rev.* **25**, 332–338 (2014).
16. B. Cao, I. U. Mysorekar, Intracellular bacteria in placental basal plate localize to extravillous trophoblasts. *Placenta* **35**, 139–142 (2014).
17. Y. Weisblum *et al.*, Modeling of human cytomegalovirus maternal-fetal transmission in a novel decidual organ culture. *J. Virol.* **85**, 13204–13213 (2011).
18. V. B. Zeldovich, A. I. Bakardjiev, Host defense and tolerance: Unique challenges in the placenta. *PLoS Pathog.* **8**, e1002804 (2012).
19. A. C. Crespo, J. L. Strominger, T. Tilburgs, Expression of KIR2DS1 by decidual natural killer cells increases their ability to control placental HCMV infection. *Proc. Natl. Acad. Sci. U.S.A.* **113**, 15072–15077 (2016).
20. A. C. Crespo, A. van der Zwan, J. Ramalho-Santos, J. L. Strominger, T. Tilburgs, Cytotoxic potential of decidual NK cells and CD8+ T cells awakened by infections. *J. Reprod. Immunol.* **119**, 85–90 (2017).
21. A. King, P. Kalra, Y. W. Loke, Human trophoblast cell resistance to decidual NK lysis is due to lack of NK target structure. *Cell. Immunol.* **127**, 230–237 (1990).
22. H. D. Kopcow *et al.*, Human decidual NK cells form immature activating synapses and are not cytotoxic. *Proc. Natl. Acad. Sci. U.S.A.* **102**, 15563–15568 (2005).
23. O. Huhn *et al.*, How do uterine natural killer and innate lymphoid cells contribute to successful pregnancy? *Front. Immunol.* **12**, 607669 (2021).
24. A. C. Crespo *et al.*, Decidual NK cells transfer granulysin to selectively kill bacteria in trophoblasts. *Cell* **182**, 1125–1139.e18 (2020).
25. E. L. Parker, R. B. Silverstein, S. Verma, I. U. Mysorekar, Viral-immune cell interactions at the maternal-fetal interface in human pregnancy. *Front. Immunol.* **11**, 522047 (2020).
26. A. Bayer *et al.*, Type III interferons produced by human placental trophoblasts confer protection against Zika virus infection. *Cell Host Microbe* **19**, 705–712 (2016).
27. J. Corry, N. Arora, C. A. Good, Y. Sadovsky, C. B. Coyne, Organotypic models of type III interferon-mediated protection from Zika virus infections at the maternal-fetal interface. *Proc. Natl. Acad. Sci. U.S.A.* **114**, 9433–9438 (2017).
28. M. D. P. Martinez Viedma, B. E. Pickett, Characterizing the different effects of Zika virus infection in placenta and microglia cells. *Viruses* **10**, 649 (2018).
29. C. F. Chiu *et al.*, The mechanism of the Zika virus crossing the placental barrier and the blood-brain barrier. *Front. Microbiol.* **11**, 214 (2020).
30. P. G. Muthuraj *et al.*, Zika virus infection induces endoplasmic reticulum stress and apoptosis in placental trophoblasts. *Cell Death Discov.* **7**, 24 (2021).
31. M. A. Sheridan *et al.*, African and Asian strains of Zika virus differ in their ability to infect and lyse primitive human placental trophoblast. *PLoS One* **13**, e0200086 (2018).
32. Y. Hu *et al.*, IFN-gamma-mediated extravillous trophoblast outgrowth inhibition in first trimester explant culture: A role for insulin-like growth factors. *Mol. Hum. Reprod.* **14**, 281–289 (2008).

33. M. T. McMaster *et al.*, Human placental HLA-G expression is restricted to differentiated cytotrophoblasts. *J. Immunol.* **154**, 3771–3778 (1995).
34. M. Lobigs, A. Müllbacher, M. Regner, MHC class I up-regulation by flaviviruses: Immune interaction with unknown advantage to host or pathogen. *Immunol. Cell Biol.* **81**, 217–223 (2003).
35. A. Glasner *et al.*, Zika virus escapes NK cell detection by upregulating MHC class I molecules. *J. Virol.* **91**, e00785-e00717 (2017).
36. M. Petitt, T. Tabata, H. Puerta-Guardo, E. Harris, L. Pereira, Zika virus infection of first-trimester human placentas: Utility of an explant model of replication to evaluate correlates of immune protection ex vivo. *Curr. Opin. Virol.* **27**, 48–56 (2017).
37. T. Tabata *et al.*, Zika virus replicates in proliferating cells in explants from first-trimester human placentas, potential sites for dissemination of infection. *J. Infect. Dis.* **217**, 1202–1213 (2018).
38. J. Miranda *et al.*, Syncytiotrophoblast of placentae from women with Zika virus infection has altered tight junction protein expression and increased paracellular permeability. *Cells* **8**, 1174 (2019).
39. L. Ulianich *et al.*, ER stress impairs MHC class I surface expression and increases susceptibility of thyroid cells to NK-mediated cytotoxicity. *Biochim. Biophys. Acta* **1812**, 431–438 (2011).
40. D. P. Granados *et al.*, ER stress affects processing of MHC class I-associated peptides. *BMC Immunol.* **10**, 10 (2009).
41. M. Cortese *et al.*, Ultrastructural characterization of Zika virus replication factories. *Cell Rep.* **18**, 2113–2123 (2017).
42. M. I. Mohd Ropidi, A. S. Khazali, N. Nor Rashid, R. Yusof, Endoplasmic reticulum: A focal point of Zika virus infection. *J. Biomed. Sci.* **27**, 27 (2020).
43. J. P. Merlie, R. Sebbane, S. Tzartos, J. Lindstrom, Inhibition of glycosylation with tunicamycin blocks assembly of newly synthesized acetylcholine receptor subunits in muscle cells. *J. Biol. Chem.* **257**, 2694–2701 (1982).
44. M. Boyce *et al.*, A selective inhibitor of eIF2alpha dephosphorylation protects cells from ER stress. *Science* **307**, 935–939 (2005).
45. S. Sen Santara *et al.*, The NK receptor NKp46 recognizes ecto-calreticulin on ER-stressed cells. *bioRxiv* 2021.10.31.466654. https://doi.org/10.1101/2021.10.31.466654 (2 November 2021).
46. A. Kumar *et al.*, Zika virus inhibits type-I interferon production and downstream signaling. *EMBO Rep.* **17**, 1766–1775 (2016).
47. E. A. Caine, B. W. Jagger, M. S. Diamond, Animal models of Zika virus infection during pregnancy. *Viruses* **10**, 598 (2018).
48. L. J. Yockey *et al.*, Type I interferons instigate fetal demise after Zika virus infection. *Sci. Immunol.* **3**, 1247–1256 (2018).
49. R. A. Larocca *et al.*, Vaccine protection against Zika virus from Brazil. *Nature* **536**, 474–478 (2016).
50. A. Y. Collier *et al.*, Sustained maternal antibody and cellular immune responses in pregnant women infected with Zika virus and mother to infant transfer of Zika-specific antibodies. *Am. J. Reprod. Immunol.* **84**, e13288 (2020).
51. S. Rajagopalan, E. O. Long, A human histocompatibility leukocyte antigen (HLA)-G-specific receptor expressed on all natural killer cells. *J. Exp. Med.* **189**, 1093–1100 (1999).
52. G. R. Medigeshi *et al.*, West Nile virus infection activates the unfolded protein response, leading to CHOP induction and apoptosis. *J. Virol.* **81**, 10849–10860 (2007).
53. H. W. Yung *et al.*, Endoplasmic reticulum stress disrupts placental morphogenesis: Implications for human intrauterine growth restriction. *J. Pathol.* **228**, 554–564 (2012).
54. H. W. Yung *et al.*, Evidence of placental translation inhibition and endoplasmic reticulum stress in the etiology of human intrauterine growth restriction. *Am. J. Pathol.* **173**, 451–462 (2008).
55. T. Kawakami *et al.*, Prolonged endoplasmic reticulum stress alters placental morphology and causes low birth weight. *Toxicol. Appl. Pharmacol.* **275**, 134–144 (2014).
56. G. J. Burton, H. W. Yung, T. Cindrova-Davies, D. S. Charnock-Jones, Placental endoplasmic reticulum stress and oxidative stress in the pathophysiology of unexplained intrauterine growth restriction and early onset preeclampsia. *Placenta* **30 Suppl A**, S43–S48 (2009).
57. T. I. Pollin, S. I. Taylor, YIPF5 mutations cause neonatal diabetes and microcephaly: Progress for precision medicine and mechanistic understanding. *J. Clin. Invest.* **130**, 6228–6231 (2020).
58. I. Gladwyn-Ng *et al.*, Stress-induced unfolded protein response contributes to Zika virus-associated microcephaly. *Nat. Neurosci.* **21**, 63–71 (2018).
59. G. J. Burton, H. W. Yung, Endoplasmic reticulum stress in the pathogenesis of early-onset pre-eclampsia. *Pregnancy Hypertens.* **1**, 72–78 (2011).
60. C. Esk *et al.*, A human tissue screen identifies a regulator of ER secretion as a brain-size determinant. *Science* **370**, 935–941 (2020).
61. T. C. Pierson, M. S. Diamond, The emergence of Zika virus and its new clinical syndromes. *Nature* **560**, 573–581 (2018).
62. C. Alfano, I. Gladwyn-Ng, T. Couderc, M. Lecuit, L. Nguyen, The unfolded protein response: A key player in Zika virus-associated congenital microcephaly. *Front. Cell. Neurosci.* **13**, 94 (2019).
63. Q. Chen *et al.*, Metabolic reprogramming by Zika virus provokes inflammation in human placenta. *Nat. Commun.* **11**, 2967 (2020).
64. D. Vota *et al.*, Zika virus infection of first trimester trophoblast cells affects cell migration, metabolism and immune homeostasis control. *J. Cell. Physiol.* **236**, 4913–4925 (2021).
65. K. Rabelo *et al.*, Zika induces human placental damage and inflammation. *Front. Immunol.* **11**, 2146 (2020).
66. C. Megli, S. Morosky, D. Rajasundaram, C. B. Coyne, Inflammasome signaling in human placental trophoblasts regulates immune defense against *Listeria monocytogenes* infection. *J. Exp. Med.* **218**, e20200649 (2021).
67. S. F. Khaiboullina *et al.*, ZIKV infection regulates inflammasomes pathway for replication in monocytes. *Sci. Rep.* **7**, 16050 (2017).
68. Q. Shao *et al.*, Zika virus infection disrupts neurovascular development and results in postnatal microcephaly with brain damage. *Development* **143**, 4127–4136 (2016).
69. J. Lei *et al.*, IL-1 receptor antagonist therapy mitigates placental dysfunction and perinatal injury following Zika virus infection. *JCI Insight* **4**, e122678 (2019).
70. F. M. Lum *et al.*, Zika virus infection preferentially counterbalances human peripheral monocyte and/or NK cell activity. *MSphere* **3**, e00120-e00118 (2018).
71. W. Kujur *et al.*, Memory like NK cells display stem cell like properties after Zika virus infection. *PLoS Pathog.* **16**, e1009132 (2020).
72. A. A. Ashkar *et al.*, Assessment of requirements for IL-15 and IFN regulatory factors in uterine NK cell differentiation and function during pregnancy. *J. Immunol.* **171**, 2937–2944 (2003).
73. C. W. Winkler, A. B. Evans, A. B. Carmody, K. E. Peterson, Placental myeloid cells protect against Zika virus vertical transmission in a *Rag1*-deficient mouse model. *J. Immunol.* **205**, 143–152 (2020).
74. F. Gambino Jr. *et al.*, A vaccine inducing solely cytotoxic T lymphocytes fully prevents Zika virus infection and fetal damage. *Cell Rep.* **35**, 109107 (2021).
75. J. A. Regla-Nava *et al.*, Cross-reactive dengue virus-specific $CD8^+$ T cells protect against Zika virus during pregnancy. *Nat. Commun.* **9**, 3042 (2018).
76. H. Huang *et al.*, $CD8^+$ T cell immune response in immunocompetent mice during Zika virus infection. *J. Virol.* **91**, e00900–e00917 (2017).
77. A. Elong Ngono *et al.*, $CD8^+$ T cells mediate protection against Zika virus induced by an NS3-based vaccine. *Sci. Adv.* **6**, eabb2154 (2020).
78. L. Nazerai *et al.*, Effector CD8 T cell-dependent Zika virus control in the CNS: A matter of time and numbers. *Front. Immunol.* **11**, 1977 (2020).
79. A. Elong Ngono *et al.*, Mapping and role of the $CD8^+$ T cell response during primary Zika virus infection in mice. *Cell Host Microbe* **21**, 35–46 (2017).
80. C. Bartmann *et al.*, Quantification of the predominant immune cell populations in decidua throughout human pregnancy. *Am. J. Reprod. Immunol.* **71**, 109–119 (2014).
81. Z. Zhu *et al.*, Comparative genomic analysis of pre-epidemic and epidemic Zika virus strains for virological factors potentially associated with the rapidly expanding epidemic. *Emerg. Microbes Infect.* **5**, e22 (2016).
82. L. Yuan *et al.*, A single mutation in the prM protein of Zika virus contributes to fetal microcephaly. *Science* **358**, 933–936 (2017).
83. J. Siewiera *et al.*, Human cytomegalovirus infection elicits new decidual natural killer cell effector functions. *PLoS Pathog.* **9**, e1003257 (2013).